Grain-boundary chemistry and weak-link behavior of polycrystalline $YBa_2Cu_4O_8$

Z. L. Wang
Metals and Ceramics Division, Oak Ridge National Laboratory, P.O. Box 2008, Oak Ridge, Tennessee 37831 and Department of Materials Science and Engineering, The University of Tennessee, Knoxville, Tennessee 37996

J. Brynestad
Chemistry Division, Oak Ridge National Laboratory, P.O. Box 2008, Oak Ridge, Tennessee 37831

D. M. Kroeger
Metals and Ceramics Division, Oak Ridge National Laboratory, P.O. Box 2008, Oak Ridge, Tennessee 37831

Y. R. Sun
Department of Physics, The University of Tennessee, Knoxville, Tennessee 37996

J. R. Thompson
Solid State Division, Oak Ridge National Laboratory, P.O. Box 2008, Oak Ridge, Tennessee 37831 and Department of Physics, The University of Tennessee, Knoxville, Tennessee 37996

R. K. Williams
Metals and Ceramics Division, Oak Ridge National Laboratory, P.O. Box 2008, Oak Ridge, Tennessee 37831
(Received 27 April 1993)

Magnetic-susceptibility and grain-boundary-chemistry data were obtained on dense $YBa_2Cu_4O_8$ (Y 1:2:4) samples. Transmission-electron microscopy showed that the grain boundaries were free of second phases and the dislocation density was low. Cation content, oxygen composition, and hole density were determined by the combined techniques of nanoprobe energy-dispersive x-ray spectroscopy and electron-energy-loss spectroscopy. A total of 25 pairs of grains was analyzed and the results indicated that grain boundary and bulk compositions do not differ. The relative orientations of the crystallites were determined, and the results show that a wide variety of misorientations was sampled. Almost all of the grain boundaries were fully oxygenated and there are no hole deficiencies, but the magnetic-susceptibilty measurements showed that the material is granular weak linked. These results indicate that Y 1:2:4 is a material in which clean, stoichiometric boundaries still form weak links.

I. INTRODUCTION

Many potential applications of high-temperature superconductors require that the materials carry large currents in strong magnetic fields. While there appear to be good prospects for the development of helium-cooled Bi superconductors,[1] at present liquid-nitrogen-cooled materials do not carry useful amounts of current. The Y-Ba-Cu-O compounds are candidates for liquid-nitrogen-cooled applications because measurements on single-crystal films have shown that the intragranular critical current is high and does not decrease rapidly with temperature or applied field.[2] Unfortunately, soon after the discovery of $YBa_2Cu_3O_{7-x}$ (Y 1:2:3) (Ref. 3) it was established that the zero-field critical current values for polycrystalline ceramic samples were not large and were also rapidly degraded by weak magnetic fields.[4,5] The observations thus indicate that poor electrical connectivity across grain boundaries greatly reduces the conduction of supercurrents. The effect is called weak-link behavior. Understanding the original of this effect might have great practical significance and the purpose of this study was to investigate one possible explanation.

Possible sources of the effect include (1) intrinsic anisotropy of the superconducting properties and the presence of structural disorder at grain boundaries,[6,7] (2) microcracking due to thermal and transformational stresses,[8,9] and (3) the presence of nonstoichiometric material at grain boundaries.[8–11] The relationship between grain boundary chemistry and weak-link behavior is the subject of this paper.

The grain boundary chemistry of Y 1:2:3 has been the subject of a number of studies. Auger spectroscopy[2,10,12] and analytical electron microscopy[8,11,13,14] studies have shown the presence of grain boundary films and variations in copper and oxygen stoichiometry. More recently, TEM and electron-energy-loss spectroscopy (EELS)[15] have been applied to characterize the correlation between the crystallographic misorientations of the Y 1:2:3 grain boundaries and oxygen deficiency at the boundaries. This study[15] explored possible connections between weak-link behavior and oxygen nonstoichiometry at grain boundaries in Y 1:2:3 and found that oxygen deficiencies at boundaries can be related to predictions of the constrained coincidence site lattice boundary model.

In light of the tremendous impact that weak links have

0163-1829/93/48(13)/9726(9)/$06.00

on potential applications, it is essential to understand the origins of this phenomenon. A major step toward this goal is to test the applicability of any proposed mechanism to high-temperature superconductor systems other than Y 1:2:3. Such tests are particularly useful for superconductors that are chemically and structurally similar to Y 1:2:3. The compound studied in this work, $YBa_2Cu_4O_8$ (Y 1:2:4) is just such a material.

Orthorhombic Y 1:2:3 is not thermodynamically stable[16] and it has been suggested[12,16] that the grain boundary nonstoichiometry is associated with the initial stages of decomposition. $YBa_2Cu_4O_8$, another high-T_c compound (~ 80 K) of the YBCO system appears to be thermodynamically stable[17] in 1 atm oxygen pressure at temperatures below about 860 °C. Previously reported Auger spectroscopy results[18] indicated grain boundary and bulk compositions were indistinguishable for Y 1:2:4. This behavior appears different from that of Y 1:2:3. The present investigation was initiated to confirm the Auger spectroscopy measurements on Y 1:2:4 with energy dispersive x-ray spectroscopy (EDS) and EELS and to determine the effect of crystallite misorientation on the grain boundary chemistry. The weak-link behavior was also determined from susceptibility measurements.

II. SAMPLE PREPARATION AND CHARACTERISTICS

The Y 1:2:4 samples used in this study were prepared by sintering cold-pressed Y 1:2:4 powder at 1030 °C in 86 atm O_2 for 18 h. The Y 1:2:4 powder was synthesized from a Y 1:2:3-CuO composite which had been sintered for 4 h in 1 atm O_2 at 950 °C. The reason for sintering the Y 1:2:3-CuO mixture is that Y 1:2:3 is not stable in high-pressure oxygen.[16] Since decomposition is due to an oxidation reaction, one can inhibit the reaction by sintering, which limits the oxygen supply via open porosity. The Y 1:2:4 powder was formed by reacting for a total of 96 h at temperatures between 930 and 1030 °C. Oxygen pressures were decreased from 150 to 86 atm as the temperature was increased. The powder contained 263 ppm carbon, and $Ba_2Cu_3O_{6-\delta}$ (1.9 vol %), that was the only second phase detected by x-ray diffraction.

An optical micrograph of the sample is shown in Fig. 1. The TEM studies qualitatively confirmed the second phase content and also showed that the sample was quite dense. The bulk density was 92.1% of theoretical and at room temperature the electrical resistivity was 0.43 $\mu\Omega$ m. ac susceptibility data showed that T_c was about 78 K.

TEM specimens were prepared by first cutting thin 3-mm-diam disks from the bulk Y 1:2:4 material. Then the disk was polished and ground to a thickness of about 50 μm at the center of the disk. Finally, the specimen was ion milled at liquid-nitrogen temperature until a small hole was made. There were hundreds of small grains around the hole that were suitable for TEM analysis. Since the bulk Y 1:2:4 is a polycrystalline material, no preferred orientation was observed in TEM.

A typical TEM image of the Y 1:2:4 specimen is shown in Fig. 2. The grain boundaries are free of second phases, straight and structurally intact. Most of the grains contained relatively few dislocations. The nanoprobe microanalysis was performed across the boundaries.

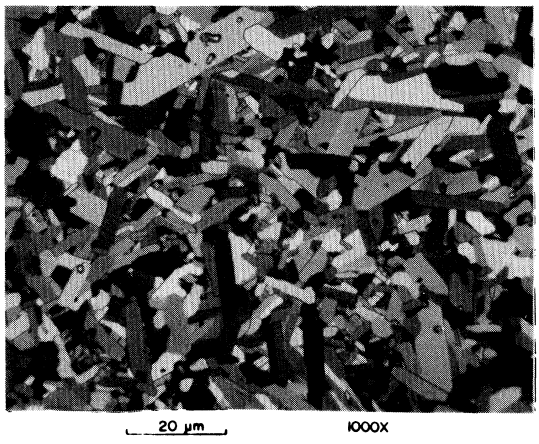

FIG. 1. Polarized light optical micrograph of the Y 1:2:4 sample.

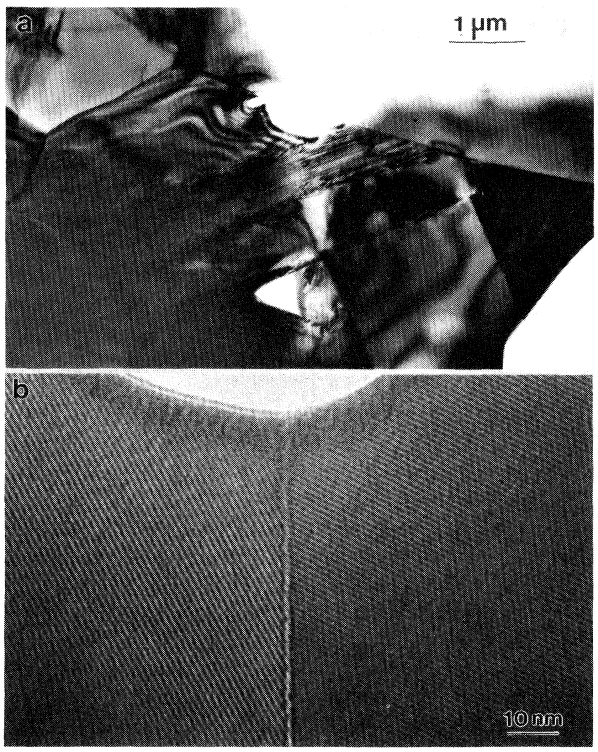

FIG. 2. TEM images of Y 1:2:4 showing clean and straight grain boundaries that have been analyzed by EELS and EDS.

III. EXPERIMENT

A. Quantitative determination of oxygen composition at grain boundaries

Transmission-electron microscopy (TEM) studies were performed at 100 kV in a Philips EM400 TEM/STEM equipped with a field emission gun (FEG). The microscope was operated in the scanning TEM (STEM) mode in order to get the smallest probe size. An electron probe of diameter less than 2 nm was generated by the FEG-TEM, and scanned across grain boundaries to detect local compositional variations. The locations of gain boundaries were directly observed in the scanning bright-field STEM images and misorientations were precisely determined with the use of microdiffraction patterns from both grains. The local chemical compositions were determined from the EDS and EELS measurements which were performed simultaneously when the electron probe was pointed at the boundary. The cation composition was determined by energy dispersive x-ray spectroscopy (EDS) and is given by[19]

$$\frac{n_a}{n_b}=\frac{k_b}{k_a}\frac{I_a}{I_b}\ , \tag{1}$$

where I_a is the integrated x-ray count for the characteristic lines of element a; n_a is the volume concentration of element a; k_a is a constant independent of n_a which depends only on the relative detection efficiency of the detector for the measured lines, ionization cross section and fluorescence yield. The three other parameters, I_b, k_b, and n_a, have similar meanings. The absorption effect is usually negligible for thin specimen microanalysis in TEM if the specimen is rotated towards the x-ray detector for about 25° in order to increase the x-ray takeoff angle. For quantitative chemical analysis, k factors must be determined experimentally from a compound of known composition. In this study, the ratios of $k_{\mathrm{Ba}}/k_{\mathrm{Cu}}$ and $k_{\mathrm{Y}}/k_{\mathrm{Cu}}$ were determined from a pure Y_2BaCuO_5 (211) phase, and the results were used to define the cation compositions in Y 1:2:4. An accuracy of better than 2% was achieved in EDS microanalysis. For 100 keV electrons, almost no contamination (or hydrocarbon deposition) was observed when the specimen was cooled below 140 K inside the TEM column in a 10^{-7} Torr vacuum.

For light elements microanalysis, EDS is not the optimum choice because of the dramatic drop of fluorescence yield for low Z elements ($Z<11$) and the unavailability of a windowless x-ray detector. These factors yield low signal counts and relatively strong background. Therefore, the oxygen composition was determined using electron-energy-loss spectroscopy (EELS), which is particularly sensitive to light elements. Figure 3 shows an EELS spectrum recorded from a Y 1:2:4 specimen. This spectrum indicates the presence of O, Ba, and Cu. After the subtraction of background, the signal intensities of the corresponding ionization edges were used to determine the specimen composition:[20]

$$\frac{n_{\mathrm{O}}}{n_{\mathrm{Ba}}}=\frac{I_{\mathrm{O}}(\beta,\Delta)}{I_{\mathrm{Ba}}(\beta,\Delta)}\frac{\sigma_{\mathrm{Ba}}}{\sigma_{\mathrm{O}}}\ , \tag{2}$$

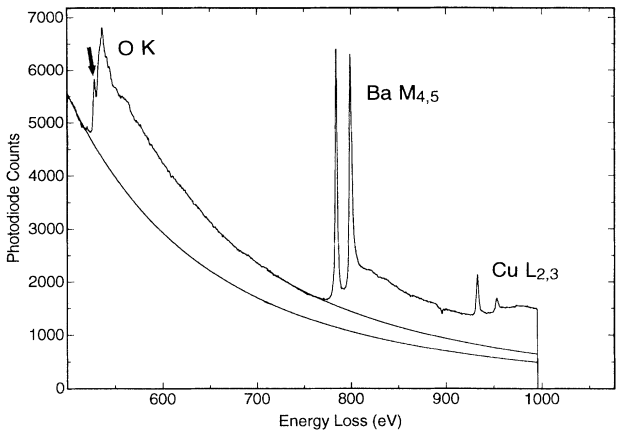

FIG. 3. A EELS spectrum acquired from a Y 1:2:4 grain showing O K, Ba $M_{4,5}$, and Cu $L_{2,3}$ edges. The pre-edge peak indicated by an arrowhead indicates the presence of unoccupied valence states (or hole states) in Y 1:2:4.

where the quantities I_{O} and I_{Ba} are the integrated intensities of the O K and Ba $M_{4,5}$ edges, respectively, for an energy window of width Δ and EELS collection semiangle β, and σ is the integrated ionization cross section of the edge. In general, it is quite inaccurate to use the calculated M-edge ionization cross section in EELS microanalysis. To avoid this problem, a standard $BaTiO_3$ sample was used to measure the $\sigma_{\mathrm{O}}/\sigma_{\mathrm{Ba}}$ ratio under equivalent experimental conditions.[21] For $\beta=25$ mrad, $\Delta=100$ eV, and $E=100$ keV, the measurements from the central transmitted beam under approximately one-beam diffracting condition showed $\sigma_{\mathrm{O}}/\sigma_{\mathrm{Ba}}=0.35\pm0.02$. This value was used in Eq. (2) to determine the O:Ba ratio in the Y 1:2:4.

Details of the experimental set up and parameter selections have been described in a previous paper on studies of Y 1:2:3.[15] The data for Y 1:2:4 were obtained under the same conditions. The EELS spectra were acquired at a dispersion of 0.5 eV/channel in order to capture both the O K and Ba $M_{4,5}$ edges. A traverse consisting of 11 EELS spectra spaced 5 nm apart was obtained for each grain boundary. It took about 6 s to acquire an EELS spectrum, but it required more than 50 s to obtain a EDS spectrum. To avoid beam damage effects, EDS spectra were acquired only on the boundary and at two positions on either side. In practice, the beam damage was not significant at 100 kV.

Kikuchi patterns were recorded from both sides of the grain boundaries to determine the misorientation of the two adjacent grains.[22] Following the traditional method, the rotation axis is an axis around which the second grain is rotated for an angle θ in order to transform the second grain lattice axes, **a**, **b**, and **c**, to be parallel to the axes **a**′, **b**′, and **c**′, respectively, of the first grain.[23,24] The minimum rotation angle about the axis with positive sense was chosen to describe the misorientation of the boundary. The boundary misorientation angle θ is determined from the indexed Kikuchi patterns with the use of a computer program developed by Zhang.[25]

B. Density of unoccupied valence states at grain boundaries

In studies of $YBa_2Cu_3O_{7-x}$, it has been found that the superconducting properties strongly depend on the oxygen deficiency x ($1 \geq x \geq 0$), varying from an antiferromagnetic insulator at $x=1$, to a 90 K superconductor at $x=0$. EELS was applied to determine the effect of oxygen substoichiometry on local electronic structures in high-T_c superconductors.[26,27] For most high-T_c oxides, the O K edge is dominated by transitions of O $1s$ electrons to the conducting band which has a binding energy of 532 eV.[20] In Y 1:2:3, the binding between O and Cu atoms in the CuO_2 layers is primarily determined by the O $2p$ state and Cu $3d$ states, resulting in some unoccupied states, of p-type symmetry, in the valence band.[26–28] These holes are believed to carry supercurrent. The hole concentration in Y 1:2:3 decreases linearly with oxygen deficiency x.[29–31]

In EELS, since the states of O $1s$ electrons are almost unaffected by the binding states of the oxygen atom (i.e., the solid-state effect), the near-edge structure of the O K edge is approximately proportional to the density of states of the unoccupied valence and conducting bands. Therefore, a detailed study of O K edge fine structures can provide some information about the symmetry of the hole states. For Y 1:2:3, the hole states were found at about 4–5 eV below the conducting band, producing a pre-edge peak located at 528 eV. This pre-edge peak has also been observed for Y 1:2:4 as indicated by an arrowhead in Fig. 3. Therefore, examination of the relative intensity variation of the pre-edge peak would provide some information on the variation of hole concentration near grain boundaries in Y 1:2:4. To do this one must assume that the hole states in Y 1:2:4 are created following the same mechanism as for Y 1:2:3.

In our experiments, it was difficult to quantify the intensity of the pre-edge peak. First, since the energy resolution of EELS spectrometer is about 1.5 eV under normal data acquisition conditions, the large overlap of the pre-edge peak with the main peak, at 537 eV, makes the determination inaccurate. Second, low-energy-loss plasmon multiple scattering is always included in the spectrum, so that the sharpness of the pre-edge peak is degraded. Finally, the intensity profile of the main O K peak is unknown and it could not be simulated using a Gaussian function, giving some uncertainty in evaluating the intensity of the pre-edge peak. Therefore, the analyses of hole concentrations are qualitative.

For Y 1:2:3, the hole states have been found to have p-type symmetry and to be confined in the (001) plane.[28] Thus the intensity of the pre-edge peak depends on the direction of the electron beam relative to the c axis of the crystal. This is because the excitation probability of the peak is related to the momentum transfer of the electrons in the a-b plane. It is thus necessary to examine the dependence of the pre-edge intensity on crystal orientation. A careful assessment was initiated to select the optimum collection semiangle of the EELS spectrometer.[15] Calculations have shown that, for $\beta=25$ mrad, the contributions from all the possible momentum transfers, from scattering angles smaller than 25 mrad have been integrated during spectrum acquisition. This reduces the crystallographic orientational anisotropy of the prepeak intensity to a minimum. EELS experiments have been carried out to test this and the results are shown in Fig. 4. The intensity of the preedge peak relative to the main peak is almost unchanged when the specimen was rotated from 0° to 50° with respect to [001]. This result confirmed the validity of the parameters employed to determine the hole concentration.

In TEM, it is possible that the sample could lose oxygen under the electron beam. To assess this effect, EELS measurements were performed on an area of the specimen under the illumination of a 2-nm-diam probe for different lengths of time. The data are shown in Fig. 5. Almost no oxygen loss was observed inside the Y 1:2:4 grains. At the grain boundary, the O:Ba ratio appears to drop from 3.5 to 3 after the electron beam continuously illuminated the same area for longer than 30 s. In our experiments, however, the data acquisition for each EELS spectrum took only 6 s. This shows that there was no severe oxygen loss during EELS measurements.

C. Susceptibility measurements

The magnetic susceptibility of Y 1:2:4 was measured in order to determine whether the grain boundaries form weak links. The sample studied was nearly cylindrical, with diameter of 3.04 mm, length of 5.3 mm, and mass of 218 mg. It was mounted and installed in a magnetometer with the magnetizing field applied parallel to the cylindrical axis. A SQUID-based magnetometer (Quantum Design Model MPMS equipped with a high homogeneity 7 T magnet) provided measurements of the magnetic moment m as a function of applied magnetic field H and temperature T. To insure that the sample remained in a highly homogeneous field, we used sample scan lengths of 3 cm. Also, the magnet contained minimal trapped mag-

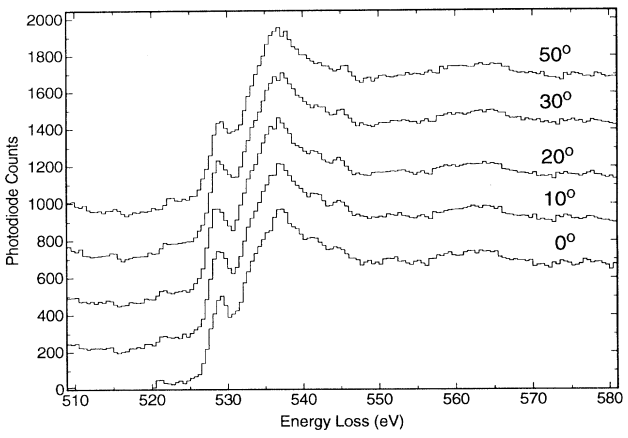

FIG. 4. A comparison of O K edge EELS spectra acquired from a same Y 1:2:4 grain when the crystal was rotated for 0°, 10°, 20°, 30°, and 50°, and 50° away from [001] zone axis, showing there is no dependence of pre-edge peak intensity on crystal orientation under the experimental conditions used here and previously (Ref. 15).

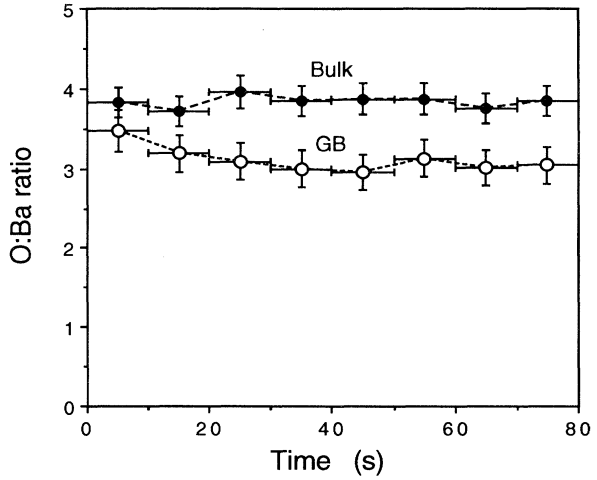

FIG. 5. Variation of O:Ba ratio on a grain boundary (GB) and in the bulk of Y 1:2:4 as a function of time when the sample was continuously illuminated by a 2-nm-diam probe, showing there is no severe oxygen-loss induced by the beam.

netic flux, since it had just been cooled to 5 K from room temperature. Meissner signals were also measured. In these experiments the sample was cooled from above T_c in an applied magnetic field.

IV. RESULTS AND DISCUSSION

A. Grain boundary chemistry determined by EDS and EELS

In previous studies of Y 1:2:3, the hole state peak was observed at some grains (about 60%) but not all. In Y 1:2:4, however, the prepeak was observed for almost every grain. This is probably associated with the fact that Y 1:2:3 shows a relatively large variation in oxygen deficiency, but the oxygen composition in Y 1:2:4 remains almost constant. For Y 1:2:4, EDS showed no significant cation compositional variation ($<2\%$) at the grain boundary and in the bulk. Thus the change of O:Ba ratio indeed reflects the variation of oxygen concentration.

As discussed previously, the hole state is actually an electronic state of the Cu-O chain in high-T_c superconductors. Two effects could cause this peak to disappear. First, oxygen deficiency could alter the peak and second, the electronic structure of Cu-O chains may be altered at some kind of boundaries. Thus the disappearance of the pre-edge peak does not necessarily mean oxygen deficiency at the boundary. The oxygen content, in practice, is determined by EELS microanalysis following Eq. (2), and hole deficiency is directly determined by the relative intensity variation of the preedge peak with respect to the main O K peak. The grain boundaries are classified into three types: fully oxygenated (FO) boundaries, hole-deficient (HD) but not oxygen deficient boundaries, and finally the oxygen deficient (OD) boundaries. It is generally true that an oxygen deficient boundary is always hole deficient.

Figure 6 shows a comparison of EELS spectra acquired at 5 nm apart across a grain boundary that is fully oxygenated. The intensity of the preedge peak does not show any significant variation either on the grain boundary (GB) or in the bulk. It can therefore be concluded that the hole concentration remains unchanged at the boundary.

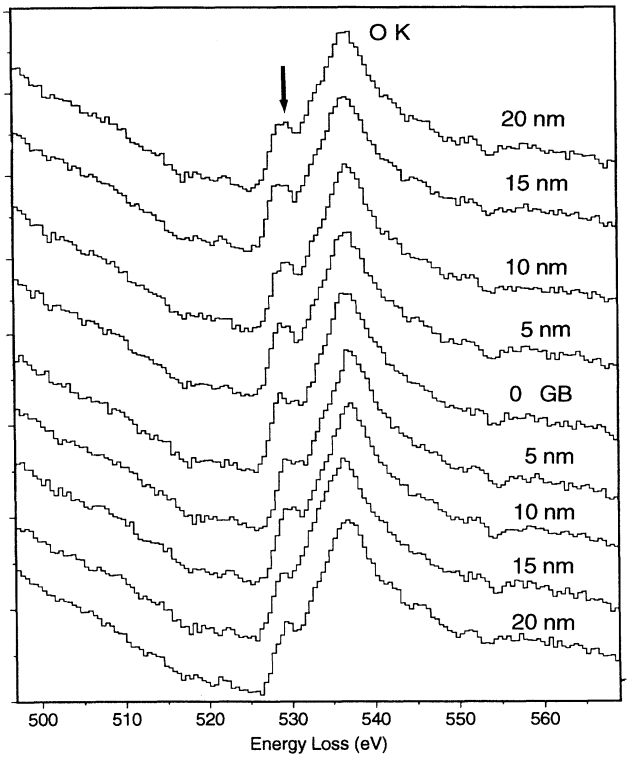

FIG. 6. A series O K edge EELS spectra acquired at 5 nm apart across a Y 1:2:4 grain boundary that is fully oxygenated, showing there are no oxygen and hole deficiency at the grain boundary.

For an oxygen deficient GB (Fig. 7), it is clear that not only does the prepeak intensity drop to a minimum, but also the magnitude of the main O K peak also drops. This boundary exhibits both oxygen deficiency and hole deficiency. Cation analysis by EDS showed that this boundary was formed between two different phases. One of the phases was Y 1:2:4 and the composition of the other phase was approximately $YBaCu_3O_y$.

To summarize the EELS and EDS analysis of many boundaries, Fig. 8(a) shows the variation of O:Ba on the boundary and in the bulk for 26 pairs of grains. The first 22 boundaries are fully oxygenated and there is no hole deficiency. The accuracy of EELS microanalysis is limited to about 5–10 %. Boundaries No. 23–25 are also fully oxygenated but show hole deficiency. Boundary No. 26, the only boundary which showed both oxygen deficiency and hole deficiency, was formed at the interface between two different phases. The EDS analyses showed that cation compositions were identical to within 3% for the two adjacent grains comprising boundaries No. 1–25.

To determine if there is any correlation between hole deficiency and grain-boundary crystallography, the

misorientation angle (or the rotation angle) was determined for each grain boundary, and the results are plotted in Fig. 8(b). The corresponding rotation axes for those boundaries are listed in Table I. For boundaries No. 1–22, which are fully oxygenated, the misorientation angles do not show any preference in either low angles or high angles and the range of angles is 3–89°. The three hole-deficient boundaries (No. 23–25) were observed for pairs of grains with misorientation angles of 31.1°, 67.1°, and 45.4°, suggesting there is no obvious correlation between boundary misorientation angle and oxygen concentration in Y 1:2:4.

B. Magnetic measurements

The magnetic studies were conducted to establish the presence or absence of weak intergrain connectivity, i.e., "weak links" between grains.[5] In the first set of measurements the sample was cooled from above T_c to 5 K in zero field (ZFC). At low temperature, a small magnetizing field in the range 2–60 G was applied, which induced a circulating supercurrent. If the induced supercurrent density J is smaller than the *intergrain* critical current density $J_{c,\text{inter}}$, then the entire sample volume is screened so that the internal flux density B is zero. The corresponding ZFC susceptibility χ is $1/4\pi$. For this low field study, we define magnetization $M=m/V$, where V is the geometrical volume of the superconductor. Then $\chi_{\text{obs}}=M/H$ is the observed dc susceptibility, measured in the applied field H. The true susceptibility, corrected for demagnetizing effects, is then $\chi=M/(H-4\pi DM)$. The demagnetizing factor D is small for the elongated geometry of the sample,[32] with an approximate value

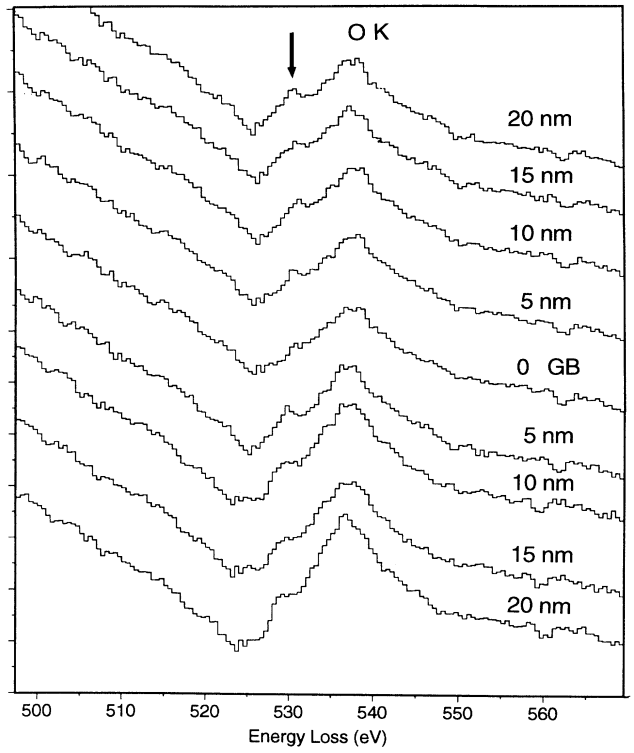

FIG. 7. A series O K edge EELS spectra acquired at 5 nm apart across a grain boundary that shows oxygen and hole deficiency. In Y 1:2:4 specimens, the oxygen deficiency was observed only for boundaries formed by two adjacent grains that are of different cation compositions.

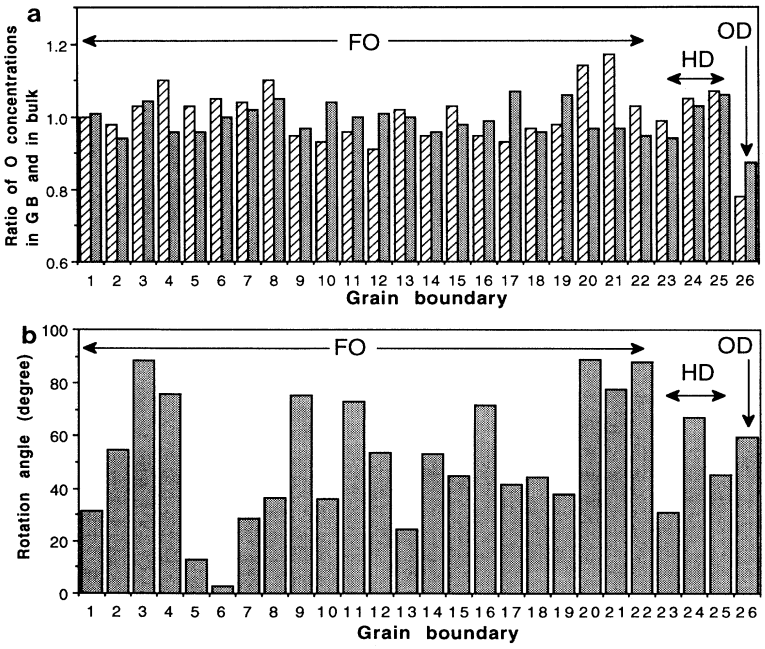

FIG. 8. (a) Ratios of oxygen concentrations on the grain boundary and in the bulk for the adjacent grains of total 26 boundaries that have been examined by EELS and EDS, showing the presence of fully oxygenated (FO), hole-deficient (HD), and oxygen-deficient (OD) boundaries (see text). (b) is a plot of the misorientation angles for the corresponding boundaries showing in (a). There appears to be no simple correlation between oxygen concentration and boundary misorientation.

TABLE I. Misorientation angles and rotation axes determined for the grain boundaries summarized in Fig. 8.

No. of GB	θ (deg)	n
1	31.4	[0.982, 0.187, 0.0]
2	54.6	[−0.985, −0.162, −0.05]
3	88.6	[0.999, 0.002, 0.05]
4	75.8	[−0.982, −0.184, −0.04]
5	12.9	[−0.543, 0.809, −0.224]
6	3.0	[1.0, 1.0, 0.0]
7	28.7	[−0.680, 0.732, 0.001]
8	36.7	[0.404, 0.904, −0.139]
9	75.6	[−0.976, −0.217, 0.0]
10	36.3	[−0.803, −0.591, −0.08]
11	73.0	[−0.599, 0.826, 0.066]
12	53.7	[−0.732, −0.679, 0.048]
13	24.7	[−0.543, 0.839, −0.02]
14	53.4	[−0.944, −0.301, −0.133]
15	44.9	[0.292, 0.804, 0.517]
16	71.9	[−0.045, −0.1, 0.08]
17	41.6	[0.378, 0.799, −0.466]
18	44.5	[−0.267, −0.565, 0.781]
19	37.9	[0.786, 0.555, −0.277]
20	89.1	[−0.808, −0.588, 0.02]
21	77.9	[−0.719, −0.694, 0.02]
22	88	[0.86, 0.494, −0.035]
23	31.1	[0.901, −0.428, −0.06]
24	67.1	[0.64, 0.77, 0.01]
25	45.4	[−0.92, −0.393, 0.01]
26	59.7	[0.772, 0.636, 0.019]

$D=0.195$ as given by Zijlstra.[33] Figure 9 shows results of the ZFC measurements versus temperature T, where plotting $4\pi\chi$ means that perfect shielding corresponds to -1. At low temperatures $T\approx 5$ K, we have $4\pi\chi=-1$ within experimental error, so the induced current flowed in the near-surface region with current density $J\leq J_{c,\text{inter}}$.

With increasing temperature, the intergrain critical current density $J_{c,\text{inter}}(T)$ decreases. When J exceeds $J_{c,\text{inter}}$, the external field penetrates the sample and $4\pi\chi$ decreases in magnitude. In the presence of weak links, this occurs at some temperature below T_c. In fact, Fig. 9 reveals a series of "knees," followed at higher temperatures by a flatter region with $4\pi\chi\approx -0.5$. This latter diamagnetism originates from screening of the interior of individual grains. This screening is incomplete, since the magnetic penetration depths λ_{ab} and λ_c have the same order of magnitude as the grain dimensions. Any sample porosity also contributes to the effect of reduced diamagnetism. Finally, at still higher temperature, we have $4\pi\chi\rightarrow 0$ at the T_c of the grains. This type of analysis is discussed more fully in a recent monograph.[34]

The presence of the knees and their strong dependence on magnetic fields give conclusive evidence for the presence of weak intergrain links. In particular, increasing the measuring field H causes the position of the knee to move rapidly downward in temperature. This is a consequence of both the well known, extreme sensitivity of $J_{c,\text{inter}}$ to small magnetic fields, along with the induction of larger currents by higher fields. Figure 10 is a plot of

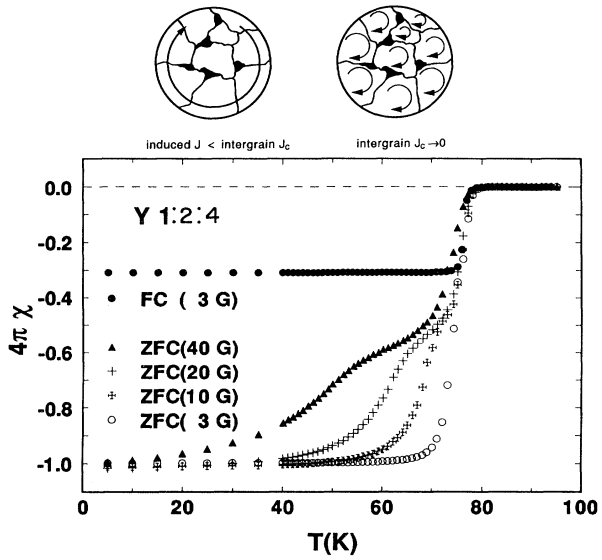

FIG. 9. Magnetic susceptibility data for the Y 1:2:4 sample. FC (3G): sample cooled to 5 K in a 3 G field. For ZFC (3G); sample cooled to 5 K in zero field, 3 G field applied, and sample warmed to $T>T_c$.

the "decoupling" field, defined by the position of the knee, versus temperature. This decoupling field increases approximately linearly as T decreases, with a slope $dH/dT\approx -1.5$ G/K. The feature can be viewed as the critical field slope for the weak links.

An explanation involving secondary superconducting phases is ruled out because apparent "T_c" (the knee) decreases with field at an unphysically high rate. This kind of explanation is also incompatible with the sample characterization data given in Sec. II. Very similar magnetic behavior was observed in polycrystalline $Tl_2Ca_2Ba_2Cu_3O_{10}$ materials, where complementary transport studies of $J_{c,\text{inter}}$ and dc characterizations were performed.[35]

Meissner signals were also investigated. When cooled

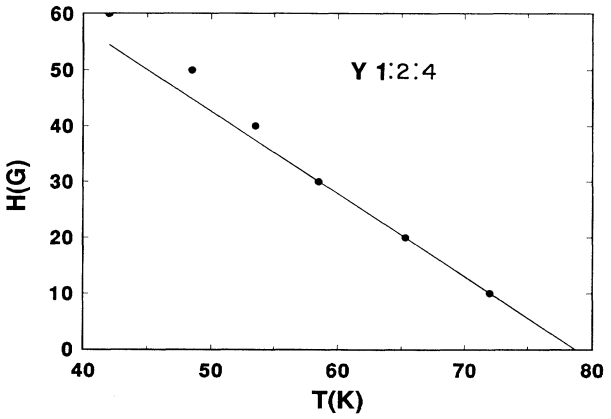

FIG. 10. Decoupling field (knee in Fig. 9) vs temperature.

from above T_c in an applied magnetic field [field cooled or (FC)], the superconductive grains expelled a portion of the magnetic flux. The bulk Meissner Effect was incomplete, giving $4\pi\chi = -0.3$ for all fields in the range 2–60 G; an example is included in Fig. 9. Reasons for the incomplete Meissner effect include flux pinning by defects within the grains; penetration of the grains near surface to depth $\sim\lambda$, where λ is the London magnetic penetration depth;[36,37] and porosity. In the FC studies, there is no structure in $4\pi\chi$ at the temperatures of the knees, as should occur if these were secondary phase superconductors. This gives further reason to reject such an explanation for the observed temperature and field dependence of the dc susceptibility.

V. CONCLUSIONS

Studies using many techniques have shown that grain boundaries in Y 1:2:3 are both nonstoichiometric and weak linked, indicating a possible relationship between boundary chemistry and critical current density. The data for Y 1:2:4 presented in this paper, however, show a different behavior. The results for Y 1:2:4 demonstrate that apparently stoichiometric grain boundaries can also form weak links between superconducting grains. It might be argued that the important compositional variation is below the limit of detection, but the data certainly show that the Y 1:2:4 boundaries are much more stoichiometric than the grain boundaries in polycrystalline Y 1:2:3.[15] The two sets of observations for Y 1:2:3 and Y 1:2:4 therefore indicate that weak-link behavior is probably an intrinsic phenomenon associated with high angle boundaries. As shown in Table I, many of the boundaries are actually high angle boundaries. The observation that boundaries covering a wide range of misorientations are all essentially stoichiometric also indicates that, at least for Y 1:2:4, grain-boundary energy has little influence on grain-boundary chemistry.

The results are also relevant to the suggestion that the hole state is associated with supercurrent formation. Hole states (or pre-edge peaks) were detected in Y 1:2:4 at virtually every point analyzed, including the grain boundaries only poorly. Since the boundaries of polycrystalline Y 1:2:4 transmit the supercurrent only poorly, the connection between the formation of hole states and supercurrent seems questionable. It is also possible that a different mechanism, which is responsible for the creation of the observed pre-edge peak, may be involved in Y 1:2:4 in comparison to that in Y 1:2:3.

It should be noted that although the magnetization measurements indicate that randomly oriented polycrystalline Y 1:2:4 is weak linked, the possibility remains that clean grain boundaries in *c*-axis oriented Y 1:2:4 may exhibit better properties than boundaries in *c*-axis oriented Y 1:2:3. Results recently reported by Masur *et al.*[38] indicate *c*-axis aligned Y 1:2:4 in multifilamentary Ag/superconductor composites prepared by an oxidation of metallic precursor process exhibited reduced weak-link behavior.

ACKNOWLEDGMENTS

The authors thank Dr. Hong Zhang for kindly providing a computer program which was used to determine grain boundary misorientations. Research was supported by the U.S. Department of Energy, Office of Advanced Utility Concepts–Superconducting Technology Program, under Contract No. DE-AC05-84OR21400 with Martin Marietta Energy Systems, Inc.

[1]K. Heine, J. Tenbrink, and M. Thoner, Appl. Phys. Lett. **55**, 2441 (1991).
[2]D. M. Kroeger, J. Metals **41**, 14 (1989).
[3]M. K. Wu, J. R. Ashburn, C. J. Torng, P. H. Hor, R. L. Meng, L. Gao, Z. J. Huang, Y. Q. Wang, and C. W. Chu, Phys. Rev. Lett. **58**, 908 (1987).
[4]R. L. Peterson and J. W. Ekin, Physica C **157**, 325 (1989).
[5]J. Clem, Physica C **153-155**, 50 (1988).
[6]D. Dimos, P. Chaudhari, J. Mannhart, and F. K. LeGoues, Phys. Rev. Lett. **61**, 219 (1988).
[7]D. Dimos, P. Chaudhari, and J. Mannhart, Phys. Rev. B **41**, 4038 (1990).
[8]S. Nakahara, G. J. Fisanick, M. F. Yan, R. B. Van Dover, T. Boone, and R. Moore, J. Cryst. Growth **85**, 639 (1987).
[9]D. R. Clark, T. M. Shaw, and D. Dimos, J. Am. Ceram. Soc. **72**, 1103 (1989).
[10]Y. M. Chiang, J. A. S. Ikeda, and A. Roshko, in *Research Update, 1988–Ceramic Superconductor II,* edited by M. F. Yan (The American Ceramic Society, Westerville, OH, 1988), p. 607.
[11]K. B. Alexander, D. M. Kroeger, J. Bentley, and J. Brynestad, Physica C **180**, 337 (1991).
[12]D. M. Kroeger, A. Choudhury, J. Brynestad, R. K. Williams, R. A. Padgett, and W. A. Coughlan, J. Appl. Phys. **64**, 331 (1988).
[13]S. E. Babcock, T. F. Kelly, P. J. Lee, J. M. Seuntjens, L. A. LaVanier, and D. C. Larbalestier, Physica C **152**, 25 (1988).
[14]K. B. Alexander, R. K. Williams, D. M. Kroeger, and J. Brynestad, in *Ceramic Transactions,* edited by K. M. Nair, U. Balachandran, Y.-M. Chiang, and A. S. Bhalla (The American Ceramic Society, Westerville, OH, 1991), Vol. 18, p. 365.
[15]Y. Zhu, Z. L. Wang, and M. Suenaga, Philos. Mag. A **67**, 11 (1993).
[16]R. K. Williams, K. B. Alexander, J. Brynestad, T. J. Henson, D. M. Kroeger, T. B. Lindemer, G. C. Marsh, J. O. Scarbrough, and E. D. Specht, J. Appl. Phys. **70**, 906 (1991).
[17]T. B. Lindemer, F. A. Washburn, C. S. MacDougall, R. Feenstra, and O. B. Cavin, Physica C **178**, 93 (1991).
[18]R. K. Williams, J. Brynestad, T. J. Henson, D. M. Kroeger, G. C. Marsh, R. A. Padgett, and J. O. Scarbrough, J. Appl. Phys. **69**, 2426 (1991).
[19]G. Cliff and G. W. Lorimer, J. Microsc. **103**, 203 (1975).
[20]R. F. Egerton, *Electron Energy-Loss Spectroscopy in the Electron Microscope* (Plenum, New York, 1986), p. 266.
[21]F. Hoffer, P. Golob, and A. Brunegger, Ultramicroscopy **25**, 81 (1988).
[22]C. T. Young, J. H. Steele, Jr., and J. L. Lytton, Metall. Trans. **4**, 2081 (1973).

[23]W. Bollmann, *Crystal Lattices, Interfaces, Matrices* (Polycrystal Bk. Serv., Dayton, OH, 1982).
[24]Y. Zhu, H. Zhang, H. Wang, and M. Suenaga, J. Mater. Res. **6**, 2507 (1991).
[25]H. Zhang, Ph.D. thesis, The State University of New York, Stony Brook, 1991 (unpublished).
[26]N. Nücker, J. Fink, J. C. Fuggle, P. J. Durham, and W. M. Temmerman, Phys. Rev. B **37**, 5158 (1988).
[27]N. Nücker, H. Romberg, X. X. Xi, J. Fink, B. Gegenheimer, and Z. X. Zhao, Phys. Rev. B **39**, 6619 (1989).
[28]J. Yuan, L. M. Brown, W. Y. Liang, R. S. Liu, and P. P. Edwards, Phys. Rev. B **43**, 8030 (1991).
[29]T. Takahashi, H. Matsuyama, T. Watanabe, H. Katayama-Yoshida, S. Sato, N. Kosugi, A. Yagishita, S. Shamoto, and M. Sato, in *Proceedings of the 3rd International Symposium on Superconductors,* edited K. Kajimura and H. Hayakawa (Springer, Berlin, 1990), p. 75.
[30]C. Y. Yang, A. R. Moodenbaugh, Y. L. Wang, Y. Xu, S. M. Geald, D. O. Welch, M. Suenaga, D. A. Fischer, and J. E. Penner-Hahn, Phys. Rev. B **42**, 2231 (1990).
[31]J. Yuan, N. Browning, and L. M. Brown, in *Proceedings of the 5th Asia-Pacific Electron Microscopy Conference,* edited by K. H. Kuo and Z. H. Zhai (World Scientific, Singapore, 1992), Vol. 1, p. 274.
[32]Note that the use of a demagnetizing factor is strictly valid only for a uniformly magnetized ellipsoid. For this superconducting sample with elongated geometry in a low magnetic field, the correction is small and the approximation is good.
[33]H. Zijlstra, *Experimental Methods in Magnetism* (North Holland, Amsterdam, 1967), p. 67.
[34]J. R. Thompson, D. K. Christen, H. R. Kerchner, L. A. Boatner, B. C. Sales, B. C. Chakoumakos, H. Hsu, J. Brynestad, D. M. Kroeger, R. K. Willims, Yang Ren Sun, Y. C. Kim, J. G. Ossandon, A. P. Malozemoff, L. Civale, A. D. Marwich, T. K. Worthington, L. Krusin-Elbaum, and F. Holtzberg, in *Magnetic Susceptibility of Superconductors and Other Spin Systems,* edited by R. A. Hein, T. Francavilla, and D. Liebenburg (Plenum, New York, 1992), pp. 157–176.
[35]J. R. Thompson, J. Brynestad, D. M. Kroeger, Y. C. Kim, S. T. Sekula, D. K. Christen, and E. D. Specht, Phys. Rev. B **39**, 6652 (1989).
[36]F. London, *Superfluids* (Dover, New York, 1961), Vol. 1.
[37]D. Schoenburg, *Superconductivity* (Cambridge University Press, Cambridge, 1960).
[38]L. J. Masur *et al.* (unpublished).

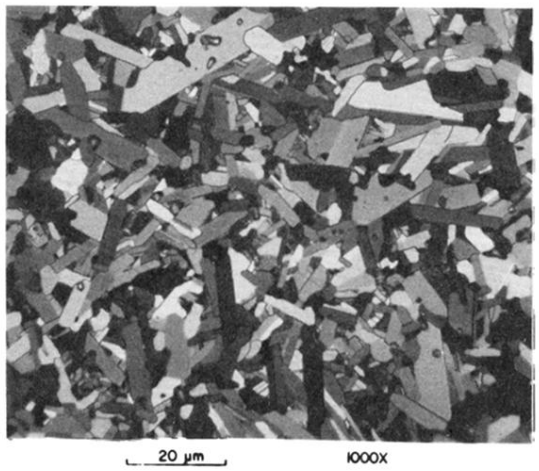

FIG. 1. Polarized light optical micrograph of the Y 1:2:4 sample.

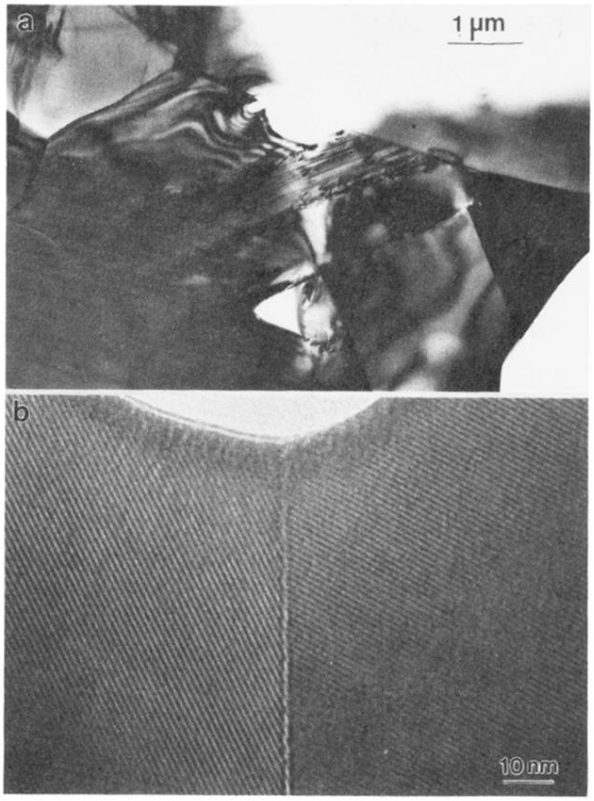

FIG. 2. TEM images of Y 1:2:4 showing clean and straight grain boundaries that have been analyzed by EELS and EDS.